

# Axially symmetric wormholes

I. A. Sarmiento-Alvarado,<sup>1,\*</sup> Leonel Bixano,<sup>1,†</sup> and Tonatiuh Matos<sup>1,‡</sup>

<sup>1</sup>*Departamento de Física, Centro de Investigación y de Estudios Avanzados del Instituto Politécnico Nacional, Av. Instituto Politécnico Nacional 2508, San Pedro Zacatenco, México 07360, CDMX.*

(Dated: February 24, 2026)

In this work, we derive an exact vacuum solution to the Einstein field equations that depends on three constant parameters: the throat radius  $r_0$ , a parameter  $q$ , which is closely associated with the Komar mass, and a parameter  $s$ , which introduces axial topological defect while avoiding the emergence of conical singularities. We employ the cut-and-paste construction to generate wormhole geometries from this solution for  $q \neq 0$ . In addition, we perform a detailed analysis of the embedding diagrams, the wormhole throat, the occurrence and structure of trapped surfaces, the behavior of geodesics, the associated tidal forces, the Petrov algebraic classification, the Newman–Penrose spin coefficients, and the corresponding invariant conserved charges.

## I. INTRODUCTION

Wormholes are among the most emblematic solutions of general relativity: spacetime configurations whose global topology allows two distant regions to be joined by a throat. Although no observations have yet confirmed their existence, they have not been ruled out in a fully model-independent way. The issue is therefore usually framed in terms of specific geometric and energetic criteria that determine when wormholes can arise and which observables might distinguish them from ordinary compact objects. The most emblematic work was done by Morris and Thorne, who emphasized the throat's geometry, an operational definition of traversability based on tidal-force limits, and the tight link between wormhole feasibility and the energy conditions [28]. In [12], Einstein and Rosen introduced the first wormhole. Later, Bronnikov and Ellis (BE) [6, 13] derived a wormhole solution by examining the EFE coupled to a scalar field. Wormhole solutions in higher dimensions have been obtained in [10, 11, 25, 32], and have also been explored in theories extending beyond General Relativity, as discussed in [3, 9, 24].

A key structural obstacle is topological censorship: in asymptotically flat, globally hyperbolic spacetimes satisfying the null energy condition, causal curves from past to future null infinity cannot access nontrivial topology [14]. This does not forbid wormholes as solutions, but it strongly restricts classical traversability under standard energy assumptions. As a result, most work proceeds along two lines: introducing matter sources that controllably violate the energy conditions or using geometric constructions that localize the nontrivial topology so that its physical and causal effects can be cleanly analyzed. A standard example of the second scenario is the cut-and-paste construction of Lorentzian wormholes, where two manifolds are glued across a timelike hypersurface and the supporting stress-energy is confined to a thin shell fixed

by the Israel junction conditions [22, 36]. Beyond providing a clean separation between bulk geometry and throat dynamics, this framework also aligns naturally with the wormhole-based formulation of cosmic censorship, which refines the standard censorship principle by insisting that any curvature singularities remain causally unreachable for physically relevant observers and geodesics [5].

From this perspective, it becomes simpler to study families of exact wormhole geometries, explicitly guided by the diagnostic criteria most relevant to traversability and censorship. Let us begin with the solution presented in [15], where the authors, Gibbons and Volkov, propose a method for constructing traversable wormholes. They obtained the Ring wormhole:

$$ds^2 = -e^{2\lambda\Phi} dt^2 + \frac{\Delta^{1+\lambda^2} [dr^2 + \Delta_r d\theta^2] + \Delta_r \sin^2 \theta d\phi^2}{e^{2\lambda\Phi}}, \quad (1)$$

where  $\Phi = \arctan \frac{r}{r_0}$ ,  $\Delta_r = r^2 + r_0^2$ ,  $\Delta_\theta = r^2 + r_0^2 \cos^2 \theta$ ,  $\Delta = \frac{\Delta_\theta}{\Delta_r}$ ,  $r_0$  is a positive constant,  $\lambda \in \mathbb{R}$  is a constant parameter,  $r \in [0, \infty)$  and  $\theta \in I_\theta = [0, \pi]$ .

The above metric has a ring singularity of radius  $r_0$ . When  $\lambda = 0$ , the wormhole throat is located at  $r = 0$  and can be viewed as a disk. In this case, the singularity encloses the disk. However, the metric (1) has not been studied for  $\lambda \neq 0$ .

In this work, we obtain an exact vacuum solution of the Einstein field equations (EFE) that includes the ring wormhole as a particular case. Our primary objective is to investigate the properties of the ring wormhole for  $\lambda \neq 0$ . The paper is organized as follows. In Section II, we derive a general solution to the EFE, and its properties are analyzed in Section III. In Section IV, we determine the Petrov classification and examine the corresponding asymptotic behavior. Subsequently, in Section V, we compute the invariant conserved charges in the sense of Komar and interpret the parameters  $q$  and  $s$ . In Section VI, we identify the trapped surfaces and the relevant spin coefficients, which are then analyzed in detail. In Section VII, we construct wormhole geometries from the obtained solution. The associated embedding surfaces are studied in Section VIII. In Section IX, we derive the conditions ensuring the existence of solutions to the

\* Contact author: ignacio.sarmiento@cinvestav.mx

† Contact author: leonel.delacruz@cinvestav.mx

‡ Contact author: tonatiuh.matos@cinvestav.mx

geodesic equations, whereas in Section X we examine the tidal forces and determine the safest region for traversing the wormhole. Finally, in Section XI, we present our concluding remarks.

## II. GENERAL SOLUTION

The Einstein field equations (EFE) in vacuum are equivalent to  $R_{\mu\nu} = 0$  for all  $\mu, \nu \in \{0, \dots, 3\}$ . If we consider a spacetime endowed with a metric  $\hat{g}$  that admits two commutative Killing vectors, then there exists a system of coordinates where the metric has the form

$$\hat{g} = \varrho[(dx^1)^2 + (dx^2)^2] + g_{ij}dx^i dx^j, \quad (2)$$

so that the EFE are reduced to

$$(vg_{,w}g^{-1})_{,\bar{w}} + (vg_{,\bar{w}}g^{-1})_{,w} = 0, \quad (3)$$

$$(\ln \varrho v^{1-1/n})_{,W} = \frac{v}{2} \text{tr}(g_{,W}g^{-1})^2 \text{ for } W \in \{w, \bar{w}\}, \quad (4)$$

where  $g = -v^{-2/n}g_{ij}$ ,  $v = \sqrt{-\det g_{ij}}$  for all  $i, j \in \{3, 4\}$ ,  $w = x^1 + ix^2$  and  $x^1 = v$ . Note that the metric components  $\varrho$  and  $g_{ij}$  depend on  $x^1$  and  $x^2$ . Consequently, the matrix  $g$  also depends on  $x^1$  and  $x^2$ . Since the determinant of  $g$  is  $\det g = -1$ ,  $g$  is a symmetric matrix in  $SL(2, \mathbb{R})$ .

Eq. (3) is a non-linear matrix differential equation and is known as the chiral equation. It solves in [33, 34] for a symmetric matrix in  $SL(n, \mathbb{R})$ , with  $n \geq 2$ . The solutions are given by

$$g(w, \bar{w}) = \exp(\zeta(w, \bar{w})A)g_0, \quad (5)$$

where  $A$  is a constant matrix in  $\mathfrak{sl}(2, \mathbb{R})$ ,  $g_0$  is a constant matrix in  $\mathcal{I}(A)$  and  $\zeta$  is a parameter that satisfies the generalized Laplace equation,

$$(v\zeta_{,w})_{,\bar{w}} + (v\zeta_{,\bar{w}})_{,w} = 0. \quad (6)$$

If Eq. (5) is considered to build an exact solution to EFE, then the field equation for the function  $F$  changes to

$$(\ln \varrho v^{1-1/n})_{,W} = \frac{v}{2} \text{tr} A^2 \zeta_{,W}^2. \quad (7)$$

In Boyer-Lindquist coordinates,  $x^1 = \sqrt{\Delta_r} \sin \theta$  and  $x^2 = r \cos \theta$ , Eq. (6) transforms to

$$(\Delta_r \zeta_{,r})_{,r} + \frac{1}{\sin \theta} (\zeta_{,\theta} \sin \theta)_{,\theta} = 0. \quad (8)$$

We solve Eq. (8) considering  $\zeta(r, \theta) = \zeta_r(r) + \zeta_\theta(\theta)$ , obtaining

$$\zeta(r, \theta) = \zeta_0 + \mathcal{C} \ln v + \frac{\mathcal{D}}{r_0} \Phi + \mathcal{E} \ln \tan \frac{\theta}{2}, \quad (9)$$

where  $\zeta_0, \mathcal{C}, \mathcal{D}, \mathcal{E} \in \mathbb{R}$ . Once we know  $\zeta$ , we can determine  $\varrho$ . To do it, we solve Eq. (7) in Boyer-Lindquist coordinates,

$$\begin{aligned} (\ln \varrho v^{1-1/n})_{,r} &= \frac{\text{tr} A^2}{4} \frac{r \sin^2 \theta}{\Delta} \left( \zeta_{,r}^2 + \frac{2 \cot \theta \zeta_{,r} \zeta_{,\theta}}{r} - \frac{\zeta_{,\theta}^2}{\Delta_r} \right), \\ (\ln \varrho v^{1-1/n})_{,\theta} &= \frac{\text{tr} A^2}{-8} \frac{\sin 2\theta}{\Delta} \left( \zeta_{,r}^2 - \frac{2r \tan \theta \zeta_{,r} \zeta_{,\theta}}{\Delta_r} - \frac{\zeta_{,\theta}^2}{\Delta_r} \right). \end{aligned} \quad (10)$$

Then,  $\varrho$  is given by

$$\varrho(r, \theta) = \mathcal{F} v^{\mathfrak{a}} \tan^{\mathfrak{c}} \frac{\theta}{2} \Delta^{\mathfrak{d}} \Xi^{\mathfrak{f}} \exp(\mathfrak{b}\Phi + \mathfrak{e}\Theta), \quad (11)$$

where  $\Xi = \frac{\sin^2 \theta}{\Delta_\theta}$ ,  $\Theta = \arctan(\frac{r}{r_0} \sec \theta)$ ,  $\mathcal{F}$  is a positive constant,  $\mathfrak{a} = \frac{\mathcal{C}^2}{4} \text{tr} A^2 - \frac{1}{2}$ ,  $\mathfrak{b} = \frac{\mathcal{C}\mathcal{D}}{2r_0} \text{tr} A^2$ ,  $\mathfrak{c} = \frac{\mathcal{C}\mathcal{E}}{2} \text{tr} A^2$ ,  $\mathfrak{d} = \frac{\mathcal{D}^2}{8r_0^2} \text{tr} A^2$ ,  $\mathfrak{e} = \frac{\mathcal{D}\mathcal{E}}{2r_0} \text{tr} A^2$  and  $\mathfrak{f} = \frac{\mathcal{E}^2}{8} \text{tr} A^2$ .

We construct an exact solution to the EFE by considering  $A = \text{diag}(1, -1)$ . Given that  $g_0$  belongs to  $\mathcal{I}(A)$ , it has the form  $g_0 = \text{diag}(-c_0, \frac{1}{c_0})$ , where  $c_0$  is a positive constant. Furthermore, we set  $\zeta_0 = 0$ ,  $\mathcal{C} = -1$ ,  $\mathcal{D} = qr_0$ ,  $\mathcal{E} = 2s$ ,  $\mathcal{F} = 1$  and  $c_0 = 1$ . Therefore,

$$\hat{g} = -f dt^2 + \frac{\Delta^\ell h (dr^2 + \Delta_r d\theta^2) + \Delta_r \sin^2 \theta d\phi^2}{f}, \quad (12)$$

where  $f = \exp(q\Phi) \tan^{2s} \frac{\theta}{2}$ ,  $h = \Xi^{s^2} \exp(2qs\Theta)$ ,  $\ell = 1 + \frac{q^2}{4}$ ,  $q, s \in \mathbb{R}$  are constant parameters.

## III. STRUCTURE OF THE SOLUTIONS

When  $q = s = 0$ , the metric (12) reduces to

$$\hat{g} = -dt^2 + \Delta dr^2 + \Delta_\theta d\theta^2 + \Delta_r \sin^2 \theta d\phi^2, \quad (13)$$

which is the Minkowski metric in oblate spheroidal coordinates. These coordinates are related to the Cartesian coordinates as  $x = \sqrt{\Delta_r} \sin \theta \cos \phi$ ,  $y = \sqrt{\Delta_r} \sin \theta \sin \phi$  and  $z = r \cos \theta$ .

The metric (12) is also defined for negative values of  $r$ . We extend the values of  $r$  to the entire  $\mathbb{R}$  with the purpose of having the metric describe a wormhole. The non-negative values of  $r$  correspond to Universe 1, while the negative values correspond to Universe 2.

Now, we analyze the asymptotic behavior of the metric (12). Observe that  $h \rightarrow 0$  as  $r \rightarrow \pm\infty$ . This means that  $\hat{g}$  is not asymptotically flat when  $s \neq 0$ . Now, we assume that  $s = 0$ . Hence,

$$\hat{g} \rightarrow \frac{dr^2 + r^2 d\Omega^2}{e^{\pm q \frac{\theta}{2}}} - e^{\pm q \frac{\theta}{2}} dt^2 \text{ as } r \rightarrow \pm\infty. \quad (14)$$

Under scaling transformations:  $r \rightarrow e^{\mp q \frac{\theta}{4}} r$  and  $t \rightarrow e^{\pm q \frac{\theta}{4}} t$ , the metric (14) changes to

$$\hat{g} \rightarrow -dt^2 + dr^2 + r^2 (d\theta^2 + \sin^2 \theta d\phi^2), \quad (15)$$

which is the Minkowski metric in spherical coordinates.

In the remainder of this paper, we consider only the case  $s = 0$ . Consequently,  $h = 1$  and  $f = \exp(q\Phi)$ . Observe that the metric (12) reduces to the metric (1) with  $q = 2\lambda$ .

The Kreschman invariant, denoted by  $K$ , of the metric (12) is given by

$$K = -\frac{q^2 r_0^2}{4} \frac{\Delta_r^{2\ell-4}}{\Delta_\theta^{2\ell+1}} (R + r_0^2 S \cos^2 \theta) f^2, \quad (16)$$

where  $R(r) = -(16 + 8q^2 + q^4)r_0^4 + 6q(4 + q^2)r_0^3r - 24(2 + q^2)r_0^2r^2 + 48qr_0r^3 - 48r^4$  and  $S(r) = (16 - 4q^2 + q^4)r_0^2 + 6q(4 - q^2)r_0r + 12q^2r^2$ . The functions  $\Delta_r$  and  $f$  are positive on  $\mathbb{R}$ . However, the function  $\Delta_\theta$  is zero at  $(r, \theta) = (0, \frac{\pi}{2})$ . Since  $l$  is a positive constant,  $K$  is singular at  $(r, \theta) = (0, \frac{\pi}{2})$ .

#### IV. PETROV CLASSIFICATION

To identify the Petrov class of the spacetime, we introduced a Newman–Penrose diagonal null tetrad

$$\begin{aligned}\ell &= \frac{1}{\sqrt{2}} \left( \sqrt{-g^{tt}} \partial_t + \sqrt{g^{rr}} \partial_r \right), \\ n &= \frac{1}{\sqrt{2}} \left( \sqrt{-g^{tt}} \partial_t - \sqrt{g^{rr}} \partial_r \right), \\ m &= \frac{1}{\sqrt{2}} \left( \sqrt{g^{\theta\theta}} \partial_\theta + i \sqrt{g^{\phi\phi}} \partial_\phi \right), \\ \bar{m} &= \frac{1}{\sqrt{2}} \left( \sqrt{g^{\theta\theta}} \partial_\theta - i \sqrt{g^{\phi\phi}} \partial_\phi \right).\end{aligned}$$

Using this tetrad, we applied the usual contractions of the Weyl tensor and subsequently computed the five Newman–Penrose Weyl scalars  $\Psi_0, \dots, \Psi_4$ :

$$\begin{aligned}\Psi_0 &= -C_{abcd} \ell^a m^b \ell^c m^d, & \Psi_1 &= -C_{abcd} \ell^a n^b \ell^c m^d, \\ \Psi_2 &= -C_{abcd} \ell^a m^b \bar{m}^c n^d, & \Psi_3 &= -C_{abcd} \ell^a n^b \bar{m}^c n^d, \\ \Psi_4 &= -C_{abcd} \bar{m}^a n^b \bar{m}^c n^d,\end{aligned}$$

where  $C_{abcd}$  is the Weyl tensor.

In our analysis, all five scalars are listed in Appendix B, so we can see that all the scalars  $\Psi \neq 0$ . We then formed the usual algebraic invariants

$$\mathcal{I} = \Psi_0\Psi_4 - 4\Psi_1\Psi_3 + 3\Psi_2^2, \quad \mathcal{J} = \det \begin{pmatrix} \Psi_4 & \Psi_3 & \Psi_2 \\ \Psi_3 & \Psi_2 & \Psi_1 \\ \Psi_2 & \Psi_1 & \Psi_0 \end{pmatrix}. \quad (17)$$

These are both nonzero for generic choices of the parameters and coordinates. In addition, we obtain  $\mathcal{I}^3 \neq 27\mathcal{J}^2$ , implying that the Weyl tensor is algebraically general (Petrov type I) according to the standard invariant classification [17, 30, 31, 38]. The explicit formulas for the invariants  $\mathcal{I}$  and  $\mathcal{J}$  are in the Appendix B, instead, in the next subsection we will discuss the asymptotic behaviour of the NPW scalars.

##### A. Asymptotic Weyl scalars and physical interpretation

Throughout all subsequent paragraphs, reference will be made to Appendix B.

*a. Coulomb term and effective mass.* The leading decay behavior  $\Psi_2 \sim r^{-3}$  corresponds to the usual Coulomb-type falloff of the Weyl tensor for asymptotically isolated systems. More precisely, in the standard asymptotic normalization one finds  $-\Psi_2 \sim -M/r^3 + \dots$  for a pure mass

monopole. Comparing this with  $\lim_{r \rightarrow \pm\infty} \Psi_2$  one can define an effective monopole mass

$$M_{\text{eff}} \sim \pm \frac{qr_0}{2} f_{\pm\infty}, \quad (18)$$

it is intimately connected to the Komar mass  $M_K$  that will be computed in the next section V. Under a wormhole interpretation, this implies that both asymptotic regions perceive the same mass parameter. At large distances from the throat, the Weyl tensor is thus primarily governed by a Coulomb-type (monopolar) tidal component described by  $\Psi_2$ , while the higher-order multipole tidal contributions, given by  $\Psi_{0,1,3,4}$ , diminish more rapidly and can be neglected.

*b. Absence of gravitational radiation.* A genuinely radiative outgoing part would appear as a leading  $\Psi_4 \sim r^{-1}$  term at null infinity. However,  $\lim_{r \rightarrow \pm\infty} \Psi_4$  instead yields  $\Psi_4 \sim \mathcal{O}(r^{-5})$ , which is far too suppressed to describe a true gravitational-wave flux. This agrees with the fact that the solution is stationary. Similarly, the equality  $\Psi_0 = \Psi_4$  indicates a symmetry between ingoing and outgoing null directions in the chosen tetrad, rather than signaling actual radiation.

*c. Higher multipoles and axial angular structure.* The scalars  $\Psi_0$  and  $\Psi_1$  fall off as  $r^{-5}$  and exhibit explicit angular dependence via  $\sin^2\theta$  and  $\sin(2\theta)$ , which is typical of axisymmetric higher-multipole (tidal) structure rather than radiative modes. An important indicator is that the multipolar corrections are reduced by two additional powers of  $r$  compared to the Coulomb term at the infinity:

$$\frac{|\Psi_0|}{|\Psi_2|} \sim \frac{(q^2 + 4)r_0^2}{8r^2} \sin^2\theta, \quad \frac{|\Psi_1|}{|\Psi_2|} \sim \frac{(q^2 + 4)r_0^2}{16r^2} |\sin(2\theta)|. \quad (19)$$

Thus, at large distances the monopole contribution contained in  $\Psi_2$  is dominant, whereas the  $\mathcal{O}(r^{-5})$  terms represent progressively smaller multipole corrections.

*d. Consistency with Petrov type and wormhole interpretation.* Independently of the asymptotic analysis above, the algebraic type is determined by the curvature invariants: because  $\mathcal{I}^3 \neq 27\mathcal{J}^2$ , the spacetime is algebraically general (Petrov type I). The conditions  $\Psi_0 = \Psi_4$  and  $\Psi_3 = -\Psi_1$  do not indicate algebraic speciality, instead, they are compatible with a discrete symmetry that interchanges ingoing and outgoing null directions, as one would expect in a stationary wormhole spacetime with two equivalent asymptotic universes. In the limit  $r \rightarrow \pm\infty$ , the fact that  $\Psi_2$  dominates shows that the Weyl tensor tends toward a Coulomb-type behavior, whereas the local structure near the throat remains algebraically general.

*e. Minkowski limit.* By setting the parameter  $q = 0$  in our NPW invariants, we observe that all invariants  $\Psi$  vanish,  $\Psi = 0$ . Consequently, we recover the well-known Minkowski space-time expressed in Boyer–Lindquist coordinates, as previously discussed in Section II. Therefore, this solution is well behaved, and the Minkowski limit is obtained in the case where the *effective mass monopole parameter*  $q$  is switched off.

*f. Asymptotic Petrov character.* Although the invariant condition  $\mathcal{I}^3 \neq 27\mathcal{J}^2$  indicates that the spacetime is, in general, algebraically generic (Petrov type I), the asymptotic behavior  $\Psi_2 \sim \mathcal{O}(r^{-3})$  together with  $\Psi_0, \Psi_1, \Psi_3, \Psi_4 \sim \mathcal{O}(r^{-5})$  implies that, in the limit  $r \rightarrow \pm\infty$ , the curvature invariants are dominated by the Coulomb-like contribution. In particular, one finds  $\mathcal{I} = 3\Psi_2^2 + \mathcal{O}(r^{-10})$ ,  $\mathcal{J} = -\Psi_2^3 + \mathcal{O}(r^{-13})$ . Equivalently, by taking the asymptotic limits of  $\mathcal{I}$  and  $\mathcal{J}$ , we recover Eq. (61). This relation shows that the geometry becomes *asymptotically* of Petrov type D, even though it remains of type I in the strong-field region ( $r \ll \pm\infty$ ).

## V. KOMAR MASS AND KOMAR ANGULAR MOMENTUM

In this section, we compute the invariant conserved charges using the results presented in Appendix A. The mass  $M$  is determined from the Komar integral associated with the stationary Killing vector  $\partial_t$ , following Komar's original prescription [23, 29]. The angular momentum  $J$  is obtained as the Komar charge corresponding to the axial Killing vector  $\partial_\varphi$  [8, 23, 29].

Let  $\xi = \partial_t$  and  $\eta = \partial_\phi$  denote the stationary and axial Killing vector fields, respectively. Their associated one-forms are given by  $\xi^b = g(\xi, \cdot) = g_{tt} dt$  and  $\eta^b = g(\eta, \cdot) = g_{\phi\phi} d\phi$ . Using these, we introduce the Komar mass and Komar angular momentum as follows:

$$M_K = -\frac{1}{8\pi} \int_{S_r} \star d\xi^b, \quad J_K = \frac{1}{16\pi} \int_{S_r} \star d\eta^b. \quad (20)$$

The overall sign in  $M_K$  is chosen in the standard way so that, in the usual gauge, one has  $M_K > 0$  for the Schwarzschild solution.

Let us start by taking the exterior derivative of the 1-form  $\eta^b$

$$d\eta^b = \partial_r(g_{\phi\phi}) dr \wedge d\phi + \partial_\theta(g_{\phi\phi}) d\theta \wedge d\phi.$$

We observe that there is no  $tr$  component, i.e.  $(d\eta^b)_{tr} = 0$ . Therefore, to compute the Komar angular momentum (20), we apply (56). However, using  $H_{tr} = (d\eta^b)_{tr}$  in (55), it follows that, for this particular solution,

$$J_K = 0. \quad (21)$$

On the other hand, we find that  $d\xi^b = -df \wedge dt = \partial_r f dt \wedge dr + \partial_\theta f dt \wedge d\theta$ . Hence, by (55), the only term that contributes to  $H_{tr}$  is  $(d\xi^b)_{tr} = \partial_r f$ . Substituting in (55)

$$(\star d\xi^b)_{\theta\phi} = -\Delta_r \sin\theta \frac{\partial_r f}{f} = -\Delta_r \sin\theta \partial_r(\ln f),$$

introducing in (20)

$$\begin{aligned} M_K(r) &= -\frac{1}{8\pi} \int_0^{2\pi} d\phi \int_0^\pi d\theta (\star d\xi^b)_{\theta\phi} \\ &= \frac{1}{8\pi} \int_0^{2\pi} d\phi \int_0^\pi d\theta \Delta_r \sin\theta \partial_r(\ln f) \\ &= \frac{1}{4} \int_0^\pi \Delta_r \sin\theta \left( q \frac{r_0}{\Delta_r} \right) d\theta = \frac{q r_0}{4} \int_0^\pi \sin\theta d\theta \\ &= \frac{q r_0}{2}, \end{aligned} \quad (22)$$

where  $\ln f = q\Phi(r) + 2s \ln \tan \frac{\theta}{2}$ , then  $\partial_r(\ln f) = q\Phi'(r)$ , and  $\Phi'(r) = \frac{r_0}{r^2 + r_0^2} = \frac{r_0}{\Delta_r}$ . Therefore the Komar mass at infinity is

$$M_\infty = \lim_{x \rightarrow \infty} M_K(r) = \frac{q r_0}{2}. \quad (23)$$

These results enable us to state with greater confidence that our spacetime is static, since there is no frame dragging and the azimuthal component of the flow vanishes, as shown in (21). Furthermore, from (23) it is clear that the parameter  $q$  determines whether the mass is positive or negative, and this expression is independent of the parameter  $s$ . However, we must proceed with caution, because this parameter governs the asymptotic behaviour.

*a. The disappearance of the NUT parameter.* The twist or vorticity associated with  $\xi$  is the 1-form

$$\omega = \star(\xi^b \wedge d\xi^b)$$

which provides an entirely geometric characterization of how  $\xi$  fails to be hypersurface-orthogonal. In fact, by the Frobenius theorem,  $\xi$  is hypersurface-orthogonal (equivalently, the spacetime is static in coordinates adapted to  $\xi$ ) if and only if  $\xi^b \wedge d\xi^b = 0$ , i.e., if and only if  $\omega = 0$ . For our diagonal metric one has  $d\xi^b = -df \wedge dt$  and therefore  $\xi^b \wedge d\xi^b = f dt \wedge df \wedge dt = 0$ , therefore  $\omega = 0$ .

The NUT charge is defined as the monopole (Gauss) flux of the twist across a large 2-sphere,  $N \propto \int_{S_\infty} \omega$ . Consequently, for our solution the NUT charge is zero:

$$N = 0. \quad (24)$$

*b. Parameter  $s$*  Let  $S_x$  be the surface defined in Appendix A, and consider the induced 2-metric in coordinates  $(\theta, \phi)$ ,  $d\sigma^2 = g_{\theta\theta} d\theta^2 + g_{\phi\phi} d\phi^2$ . With  $A = \Delta^\ell h$ , a standard axis regularity test compares the azimuthal circumference  $C = 2\pi\sqrt{g_{\phi\phi}}$  with the proper meridional distance  $\rho = \int_0^\theta \sqrt{g_{\theta\theta}} d\theta'$ . For a conical axis one finds  $C = 2\pi\alpha\rho(\theta) + o(\rho)$  with finite  $\alpha = \lim_{\theta \rightarrow 0} \frac{C}{2\pi\rho} \in (0, \infty)$ , leading to an angular deficit  $\delta = 2\pi(1 - \alpha)$  [27, 35].

Now taking into account, for example, the north pole axis  $\theta \rightarrow 0$

$$\sin\theta \sim \theta, \quad \Delta_\theta \rightarrow r^2 + r_0^2 = \Delta_r, \quad \left( \frac{\Delta_\theta}{\Delta_r} \right)^\ell \rightarrow 1$$

therefore

$$A \sim \Delta_r^{-s^2} e^{2qs\Phi(r)} \theta^{2s^2} \implies A \xrightarrow[\theta \rightarrow 0]{} 0 \text{ if } s \neq 0.$$

Consequently,

$$g_{\theta\theta} \propto A(\theta) \sim \theta^{2s^2}, \quad g_{\phi\phi} \sim \sin^2 \theta \sim \theta^2,$$

which yields

$$\rho \propto \int_0^\theta \theta' s^2 d\theta' \propto \theta^{1+s^2}, \quad C \propto \theta,$$

$$\therefore \frac{C}{2\pi\rho} \propto \theta^{-s^2} \rightarrow \infty \quad (s \neq 0).$$

Thus, for  $s \neq 0$ , the pole is not merely conical defect, instead, the parameter  $s$  controls the axial/polar geometry. Consequently,  $s \neq 0$  generates an *axis singularity that is stronger than a conical defect*, meaning it cannot be interpreted as a simple cosmic-string-like deficit angle.

## VI. TRAPPED AND MARGINALLY TRAPPED SURFACES

For our porpouse, we will employ a geometrically preferred NP tetrad constructed from the static Killing field, first we select the unit future-directed 4-velocity field of static observers, given by:

$$u^\mu := \frac{\xi^\mu}{\sqrt{-\xi^2}}, \quad | \quad u^\mu u_\mu = -1, \quad (25)$$

where  $\xi = \partial_t$  and  $\xi^2 = \xi^\mu \xi_\mu$ , and, by selecting the orthogonal proper acceleration  $u^\nu \nabla_\nu u_\mu$  and subsequently normalizing it, we obtain

$$s^\mu = \frac{a^\mu}{\sqrt{a^\mu a_\mu}}, \quad (26)$$

fulfilling  $a^\mu u_\mu = 0$  and  $a^\mu a_\mu = 1$ .

The second step is to construct two vectors that are orthogonal to both  $u^\mu$  and  $a^\mu$ . Making use of the axisymmetry of the space-time, we may select one of them as  $b^\mu = g^{\phi\phi} \partial_\phi^\mu$ . This choice guarantees that  $b^\mu b_\mu = 0$  and that  $b^\mu u_\mu = b^\mu a_\mu = 0$ . The other vector is defined by  $\widehat{e}^\mu = g^{\mu\sigma} \varepsilon_{\sigma\alpha\beta\gamma} u^\alpha s^\beta b^\gamma$ , where  $\varepsilon_{\sigma\alpha\beta\gamma}$  denotes the Levi-Civita symbol. After normalizing this vector, we obtain:

$$e^\mu = \frac{\widehat{e}^\mu}{\sqrt{\widehat{e}^\mu \widehat{e}_\mu}}, \quad (27)$$

By construction,  $e^\mu e_\mu = 1$ , and  $e^\mu u_\mu = e^\mu s_\mu = e^\mu b_\mu = 0$ .

Now, we construct the NP null tetrad as

$$\begin{aligned} l^\mu &:= \frac{1}{\sqrt{2}}(u^\mu + s^\mu), & n^\mu &:= \frac{1}{\sqrt{2}}(u^\mu - s^\mu), \\ m^\mu &:= \frac{1}{\sqrt{2}}(e^\mu + i b^\mu), & \bar{m}^\mu &:= \frac{1}{\sqrt{2}}(e^\mu - i b^\mu). \end{aligned} \quad (28)$$

These satisfy the NP inner-product relations

$$\begin{aligned} l^\mu l_\mu &= n^\mu n_\mu = m^\mu m_\mu = \bar{m}^\mu \bar{m}_\mu = 0, \\ l^\mu n_\mu &= -1, & m^\mu \bar{m}_\mu &= +1, \end{aligned}$$

with all other contractions vanishing  $l \cdot m = l \cdot \bar{m} = n \cdot m = n \cdot \bar{m} = 0$ . The construction of the NP geometrically preferred tetrad was carried out following the methodologies outlined in Refs. [1, 2, 16, 26].

For the sake of a more concise and compact notation, we introduce the following definitions. Let

$$z_N^\mu = \{l^\mu, n^\mu, m^\mu, \bar{m}^\mu\}$$

denote the geometrically preferred null Newman-Penrose tetrad, with tetrad indices  $M, N, P \in \{l, n, m, \bar{m}\}$ . We introduce the connection coefficients of the Levi-Civita connection in the null frame by

$$Z_{MNP} := z_M^\mu z_N^\nu \nabla_\mu z_{P\nu}, \quad Z_{NMP} = -Z_{NMP}. \quad (29)$$

The antisymmetry in the final two indices arises directly from metric compatibility,  $\nabla_\mu g_{\alpha\beta} = 0$ , when this condition is applied to the inner products of the tetrad vectors. The index  $M$  indicates the direction along which the derivative is evaluated, whereas  $N$  and  $P$  denote the covariant components of the tetrad.

In this notation, the Newman-Penrose spin coefficients are identified as the following components of  $Z_{MNP}$ :

$$\begin{aligned} \kappa &= Z_{lml}, & \sigma &= Z_{mml}, \\ \rho &= Z_{\bar{m}ml}, & \tau &= Z_{nml}, \\ \pi &= -Z_{l\bar{m}n}, & \mu &= Z_{\bar{m}mn}, \\ \lambda &= Z_{\bar{m}\bar{m}n}, & \nu &= Z_{n\bar{m}n}, \\ \epsilon &= \frac{1}{2}(Z_{lnl} - Z_{l\bar{m}m}), & \gamma &= \frac{1}{2}(Z_{nln} - Z_{nm\bar{m}}), \\ \alpha &= \frac{1}{2}(Z_{\bar{m}nl} - Z_{\bar{m}\bar{m}m}), & \beta &= \frac{1}{2}(Z_{mln} - Z_{mm\bar{m}}). \end{aligned} \quad (30)$$

In our situation, we find

$$\kappa = \pi = -\tau = -\nu = -\frac{\ell r_0^2 \sqrt{f} \sin \theta \cos \theta}{2\sqrt{2} \sqrt{\Delta^\ell} \Delta_r \Delta_\theta}, \quad (31a)$$

$$\sigma = \lambda = -\frac{\ell r_0^2 \sqrt{f} r \sin^2 \theta}{2\sqrt{2} \sqrt{\Delta^\ell} \Delta_\theta \Delta_r}, \quad (31b)$$

$$\begin{aligned} \rho = \mu &= \frac{\sqrt{f}}{2\sqrt{2} \sqrt{\Delta^\ell} \Delta_\theta \Delta_r} \left( r_0^2 \cos^2 \theta ((\ell - 2)r + qr_0) \right. \\ &\quad \left. - r(\ell r_0^2 - qr_0 r + 2r^2) \right), \end{aligned} \quad (31c)$$

$$\epsilon = \gamma = -\frac{qr_0 \sqrt{f}}{4\sqrt{2} \sqrt{\Delta^\ell} \Delta_r}, \quad (31d)$$

$$\alpha = -\beta = \frac{\sqrt{f}}{2\sqrt{2} \tan \theta \sqrt{\Delta^\ell} \Delta_r}. \quad (31e)$$

By analyzing (31), we observe that in all cases the spin coefficients are purely real, in other words,  $\Im(Z_{MNP}) = 0$ . Adopting the purely geometric interpretation of these coefficients, the complex optical scalars associated with

the null congruences generated by  $l^\mu$  and  $n^\mu$  are encoded in (31c) in the following manner:

$$\begin{aligned} \rho &= \underbrace{\Re(\rho)}_{\text{expansion of } l} + i \underbrace{\Im(\rho)}_{\text{twist of } l}, \\ \mu &= \underbrace{\Re(\mu)}_{\text{expansion of } n} + i \underbrace{\Im(\mu)}_{\text{twist of } n}. \end{aligned}$$

Consequently, *the null congruences are non-twisting (i.e., hypersurface-orthogonal)*. This aligns with the static nature of the spacetime. In a static region there is no frame dragging, and one can select the transverse frame so that no spurious phase rotation appears in  $m^\mu$ .

*a. Important caveat (geodesic/affine conditions).* Even though our adapted null normals are twist-free, they are *not required* to be geodesic or affinely parametrised. Specifically, the conditions  $\kappa \neq 0$  and/or  $\epsilon + \bar{\epsilon} \neq 0$  signal that  $l^\mu$  is not a geodesic generator and/or is not affinely parametrised.

*b. 2-surfaces and induced metric.* We now employ this decomposition to examine trapped and marginally trapped surfaces, as well as potential wormhole throats. Let  $S$  be a spacelike 2-surface in the space-time manifold. Given future-directed null normal vectors  $l^\mu$  and  $n^\mu$ , orthogonal to  $S$  and normalized such that  $l \cdot n = -1$ , the induced metric (i.e., the projection tensor) on the tangent bundle  $TS$  is given by

$$q_{\mu\nu} := g_{\mu\nu} + l_\mu n_\nu + n_\mu l_\nu, \quad | \quad q^\mu{}_\nu l^\nu = q^\mu{}_\nu n^\nu = 0.$$

*c. Null expansions (covariant definition).* The outgoing/ingoing null expansions are defined quasi-locally by

$$\theta_{(l)} = q^{\mu\nu} \nabla_\mu l_\nu, \quad \theta_{(n)} = q^{\mu\nu} \nabla_\mu n_\nu.$$

These definitions are purely geometric and do *not* require  $l^\mu$  or  $n^\mu$  to be geodesic.

*d. Relation to NP coefficients.* If  $m^\mu$  and  $\bar{m}^\mu$  span the tangent space of  $S$ , then  $q^{\mu\nu} = 2m^{(\mu}\bar{m}^{\nu)}$ . In this case, the expansions are directly related to the NP optical scalars:

$$\theta_{(l)} = -(\rho + \bar{\rho}) = -2\Re(\rho), \quad (32)$$

$$\theta_{(n)} = -(\mu + \bar{\mu}) = -2\Re(\mu). \quad (33)$$

In our solution  $\rho, \mu \in \mathbb{R}$ , hence  $\theta_{(l)} = \theta_{(n)} = -2\rho$ .

*e. Trapped and marginally trapped surfaces.* A spacelike 2-surface  $S$  is said to be (future) trapped if

$$\theta_{(l)} < 0 \quad \text{and} \quad \theta_{(n)} < 0, \quad (34)$$

everywhere on  $S$ . A marginally outer trapped surface (MOTS) satisfies

$$\theta_{(l)} = 0, \quad \theta_{(n)} < 0, \quad (35)$$

with the external condition determined by the selected orientation, that is, by which null normal is designated as

outgoing. In our case, only the condition specified in (34) can be satisfied. Taking into account  $r > 0$  and  $q > 0$ , we found that the region where  $\theta_{(l)} = -2\rho < 0$  appears when  $0 < \frac{r}{r_0} < \frac{q}{2}$ .

All the formalism developed in this section is formulated on the basis of the foundational works [18–21, 30].

## VII. WORMHOLES

In this section, we will construct wormholes using the solution (12) with  $s = 0$ .

Let

$$\hat{g}_\perp = \Delta^\ell d\theta^2 + \sin^2 \theta d\phi^2. \quad (36)$$

Here,  $\Delta = 1 - \epsilon_0^2 \sin^2 \theta$  and  $\epsilon_0 = \frac{r_0}{\sqrt{\Delta r}} \in (0, 1]$  with  $r = \text{const}$ . It has the Killing vector  $\partial_\phi$ . If  $r \rightarrow \pm\infty$ , then  $\epsilon_0 \rightarrow 0$ , so that  $\hat{g}_\perp \rightarrow d\theta^2 + \sin^2 \theta d\phi^2$ , which is the metric of a 2-sphere. We assume that the metric (36) corresponds to a surface of revolution embedded in the Euclidean space  $\mathbb{R}^3$  parametrized by  $(\phi, \theta) \mapsto (\rho(\theta), \phi, z(\theta))$ . Then,

$$\hat{g}_\perp = dz^2 + d\rho^2 + \rho^2 d\phi^2 = (z_\theta^2 + \rho_\theta^2) d\theta^2 + \rho^2 d\phi^2 \quad (37)$$

Comparing Eqs. (36) and (37), we have  $\rho = \sin \theta$  and  $z_\theta^2 = \Delta^\ell - \cos^2 \theta$ . Using  $\Delta^\ell \geq 1 - \ell\epsilon_0^2 \sin^2 \theta$ , we get  $z_\theta^2 \geq (1 - \ell\epsilon_0^2) \sin^2 \theta$ . If  $\epsilon_0 \leq \frac{1}{\sqrt{\ell}}$ , then  $z_\theta^2 \geq 0$ .

Let

$$\mathcal{A}_\perp(\epsilon_0) = 2\pi \int_0^\pi \sqrt{\Delta^\ell} \sin \theta d\theta \quad (38)$$

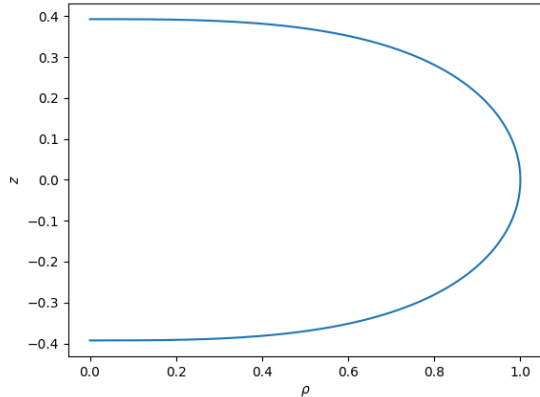
be the area given by the metric (36). Let  $\Delta_\ell = \Delta(\epsilon_0 = \frac{1}{\sqrt{\ell}})$ . Given that  $\Delta \geq \Delta_\ell$ , then  $\mathcal{A}_\perp(\epsilon_0) \geq \mathcal{A}_\perp(\frac{1}{\sqrt{\ell}})$ . Hence,  $\mathcal{A}_\perp$  has a minimum at  $\epsilon_0 = \frac{1}{\sqrt{\ell}}$ . The surfaces with minimal area are given by the solution of  $z_\theta^2 = \Delta_\ell^\ell - \cos^2 \theta$  with the initial condition  $z(\theta = \frac{\pi}{2}) = 0$ .

If  $\ell = 1$ , then  $z = 0$  on  $I_\theta$ , so that the metric (36) corresponds to a disk of unit radius. This result agrees with that obtained by Gibbons and Volkov in [15]. When  $\ell = 2$ , the surface is parametrized by

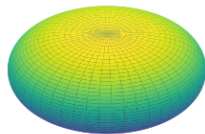
$$x = \cos \phi \sin \theta, \quad y = \sin \phi \sin \theta, \quad 8z = 2\theta - \sin 2\theta - \pi. \quad (39)$$

The image of  $z$  on  $I_\theta$  is  $[-\frac{\pi}{8}, \frac{\pi}{8}]$ . In Figure 1, we plot the shape curve and its corresponding surface of revolution for  $\ell = 2$ . Given that  $\Delta_\ell^\ell \rightarrow \exp(-\sin^2 \theta)$  as  $\ell \rightarrow \infty$ , we can define the superface of revolution given by  $z_\theta^2 = \exp(-\sin^2 \theta) - \cos^2 \theta$ . Observe in Figure 2a that  $z$  approaches 0.5 at  $\theta = 0$  and  $-0.5$  at  $\theta = \pi$ . By rotating this curve, the surface shown in Figure 2b is created. In Figure 3, we compare the shape curves for the sphere and for the surfaces with  $\ell = 1.001$  and  $\ell = 100.0$ . The shape curve tends to a line as  $\ell$  approaches 1, while it tends to curve in Figure 2a for larger values of  $\ell$ .

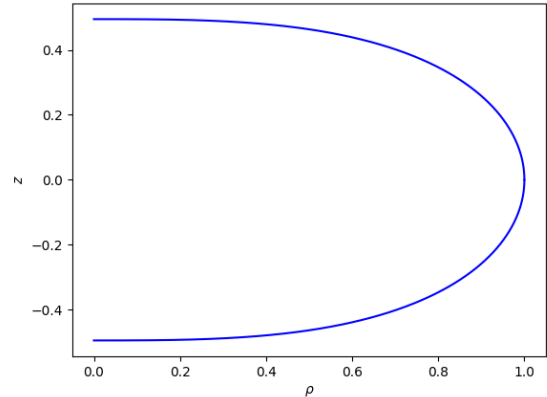
Let  $\mathcal{A} = \frac{\Delta r}{f} \mathcal{A}_\perp$  be the area of the 2-hypersurface defined by constant  $t$  and  $r$ . Inequality  $\epsilon_0 \leq \frac{1}{\sqrt{\ell}}$  implies



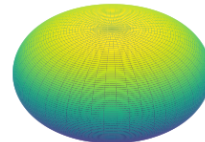
(a) Shape curve.



(b) Surface of revolution.

FIG. 1: Shape curve and its corresponding surface of revolution with  $\ell = 2$ .

(a) Shape curve.

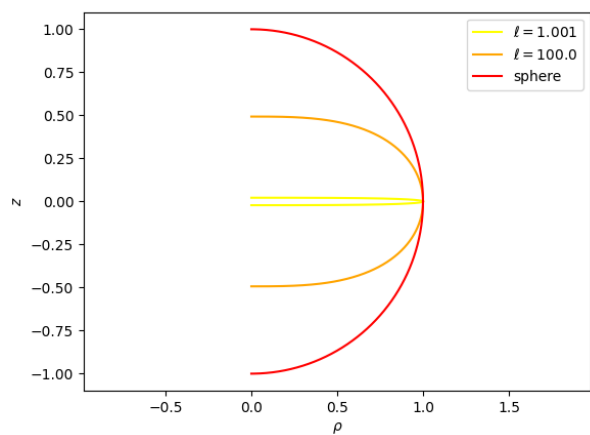


(b) Surface of revolution.

FIG. 2: Shape curve and its corresponding surface of revolution with  $\ell \rightarrow \infty$ .

$\frac{r}{r_0} \geq |\frac{q}{2}|$  or  $\frac{r}{r_0} \leq -|\frac{q}{2}|$ . Given that  $\frac{\Delta}{f}$  and  $\mathcal{A}_\perp$  has a minimum at  $r = \frac{q}{2}r_0$ ,  $\mathcal{A}$  also has a minimum at  $r = \frac{q}{2}r_0$ .

We consider a simple cut-paste construction of a wormhole [37] for  $q \neq 0$ . Let  $\mathcal{U}$  be a spacetime endowed with the metric (12) with  $s = 0$  and  $r_0 > 0$ . Let  $U_+ = \{r > \frac{q}{2}r_0 : q > 0\}$  and  $U_- = \{r < -\frac{q}{2}r_0 : q > 0\}$  be two manifolds arising from two different spacetimes  $\mathcal{U}$ . Let  $\partial U_+ = \{r = \frac{q}{2}r_0\}$  and  $\partial U_- = \{r = -\frac{q}{2}r_0\}$  be the boundaries of  $U_+$  and  $U_-$ , respectively. These manifolds are glued together by identifying their boundaries,  $\partial U_+ = \partial U_- = \partial U$ . The resulting spacetime is  $U$ . The functions  $\Delta$  and  $\Delta_r$  are the same for  $U$ ; however,  $f$  is given by  $f(r) = \exp(q \arctan(|\frac{r}{r_0}|))$ , with  $q > 0$ . Note that the metric components are continuous on  $\partial U$  and the domain of  $r$  is  $I_r = (-\infty, -\frac{q}{2}r_0] \cup [\frac{q}{2}r_0, \infty)$ . The throat of the wormhole is at  $\partial U$ . In the remaining sections, we consider the spacetime  $U$ .

FIG. 3: Shape curves for the sphere and for surfaces with  $\ell = 1.001$  and  $\ell = 100.0$ .

## VIII. THE EMBEDDING SURFACES

In this section, we will investigate the embedding surface.

Let

$$\hat{g}^{(2)} = \frac{1}{f} [\Delta^\ell dr^2 + \varepsilon_0^2 \Delta_r d\phi^2], \quad (40)$$

be the 2-dimensional hypersurface defined by constant  $t$  and  $\theta \in (0, \pi)$ . Here,  $\Delta = 1 - \varepsilon_0^2 \frac{r_0^2}{\Delta_r}$  and  $\varepsilon_0 = \sin \theta \in (0, 1]$ . This hypersurface is embedded in a 3-dimensional Euclidean space, which is parametrized by cylindrical coordinates,

$$\hat{g}^{(2)} = dz^2 + d\rho^2 + \rho^2 d\phi^2 = (z_{,r}^2 + \rho_{,r}^2) dr^2 + \rho^2 d\phi^2. \quad (41)$$

Comparing Eqs. (40) and (41), we find  $\rho = \sqrt{\frac{\Delta_r}{f}} \varepsilon_0$  and

$$z_{,r}^2 = \frac{\Delta^\ell \Delta_r - \varepsilon_0^2 (|r| - \frac{q}{2} r_0)^2}{f \Delta_r}.$$

Using the inequality  $\Delta^\ell > 1 - \ell \varepsilon_0^2 \frac{r_0^2}{\Delta_r}$ , we get

$$\Delta_r f z_{,r}^2 > (1 - \varepsilon_0^2) r^2 + q \varepsilon_0^2 r_0 |r| + (1 - \varepsilon_0^2 - \frac{q^2}{2} \varepsilon_0^2) r_0^2. \quad (42)$$

Setting  $\varepsilon_0 = 1$  into Ineq. (42), it reduces to

$$z_{,r}^2 > \frac{q r_0^2}{\Delta_r f} (|\frac{r}{r_0}| - \frac{q}{2}) \geq 0 \quad (43)$$

for all  $r \in I_r$ . If  $\varepsilon_0 < 1$ , we rewrite Ineq. (42) as

$$z_{,r}^2 > \frac{r_0^2 (1 - \varepsilon_0^2)}{f \Delta_r} (|\frac{r}{r_0}| + \frac{q}{2} \frac{1 + \varepsilon_0^2}{1 - \varepsilon_0^2}) (|\frac{r}{r_0}| - \frac{q}{2}) + \ell > 0 \quad (44)$$

for all  $r \in I_r$ .

In Figure 4a, we plot the profile curve with  $q = 2$ ,  $r_0 = 1$  and  $\theta = \frac{\pi}{2}$ . Its corresponding surface of revolution is shown in Figure 4b. Observe that the graph of profile curve is symmetric with respect to the  $\rho$ -axis, which implies that the surface is symmetric with respect to the plane  $z = 0$ .

## IX. GEODESICS

In [15], the conditions for the existence of solutions to the equations of motion with  $\theta = 0$  or  $\theta = \pi$  are found. The geodesics along the symmetry axis traverse the wormhole. In this section, we will determine the conditions for constant  $\theta \in (0, \pi)$ .

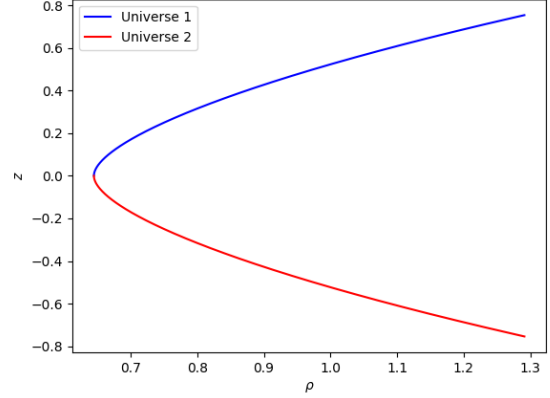
The equations of motion are obtained from the Lagrangian

$$\mathcal{L} = \frac{\Delta^\ell (\dot{r}^2 + \Delta_r \dot{\theta}^2) + \Delta_r \sin^2 \theta \dot{\phi}^2}{2f} - \frac{f}{2} \dot{t}^2, \quad (45)$$

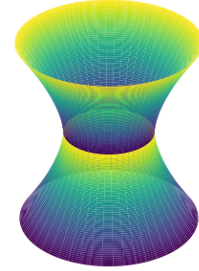
where the dot denotes the derivative with respect to the affine parameter  $\tau$ . Since  $\mathcal{L}$  does not depend on  $t$  and  $\phi$ , then  $\frac{\partial \mathcal{L}}{\partial t} = -E$  and  $\frac{\partial \mathcal{L}}{\partial \phi} = J$ , so that

$$\dot{t} = \frac{E}{f}, \quad (46)$$

$$\dot{\phi} = \frac{Jf}{\varepsilon_0^2 \Delta_r}, \quad (47)$$



(a) Profile curve



(b) Embedding surface.

FIG. 4: Profile curve and embedding surface of the wormhole with  $q = 2$ ,  $r_0 = 1$  and  $\theta = \frac{\pi}{2}$ .

where  $E$  and  $J$  are constants of integration.  $E$  can be interpreted as the energy of the system and  $J$  as the angular momentum. To avoid velocities that exceed the speed of light, we impose  $\dot{t} > 0$ . Thus,  $E > 0$ .

Combining Eq. (47) and the equation of motion for  $r$ ,

$$\Delta^\ell \dot{r}^2 = E - \frac{J^2 f^2}{\varepsilon_0^2 \Delta_r}, \quad (48)$$

we get

$$\left(\frac{dr}{d\phi}\right)^2 = \frac{\varepsilon_0^4 \Delta_r^2}{f^2 \Delta^\ell} \left(\frac{1}{b^2} - \frac{f^2}{\varepsilon_0^2 \Delta_r} + 2 \frac{J}{J^2} \mathcal{L}\right) = V_{eff}. \quad (49)$$

The effective potential  $V_{eff}$  is reduced to

$$V_{eff} = \frac{\varepsilon_0^4 \Delta_r^2}{f^2 \Delta^\ell} \left(\frac{1}{b^2} - \frac{f^2}{\varepsilon_0^2 \Delta_r}\right) \quad (50)$$

for photons  $\mathcal{L} = 0$ , where  $b = \frac{J}{E}$  is the impact parameter. Solving  $V_{eff} = V_{eff,r} = 0$ , we find the circular orbit of photons,  $r = \pm q r_0$ . The positive value corresponds to

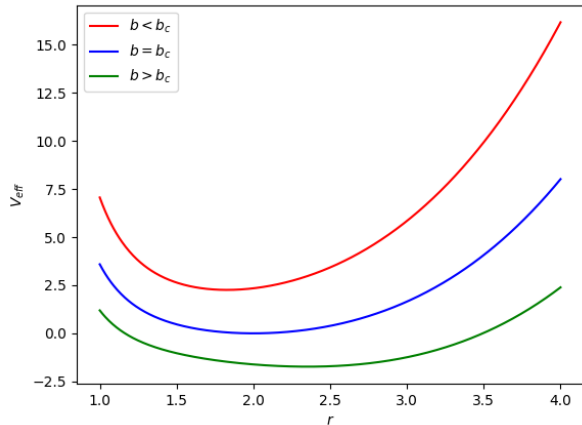


FIG. 5: Graphs of  $V_{eff}(r)$  for three values of the impact parameter  $b$ :  $b_c - 0.03$ ,  $b_c$  and  $b_c + 0.03$ . To plot them, we set  $q = 2$ ,  $r_0 = 1$  and  $\theta = \frac{\pi}{2}$ .

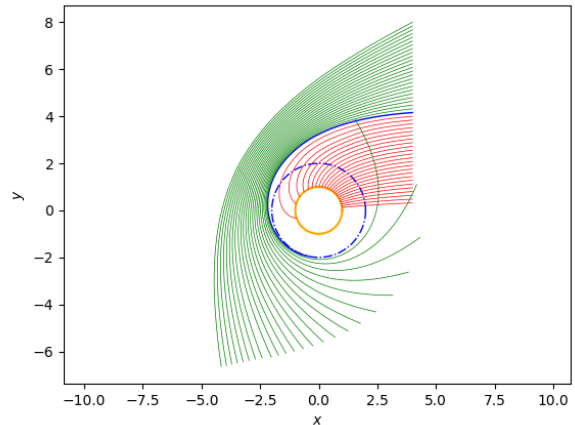


FIG. 6: Behavior of geodesics with different values of the impact parameter  $b$ . To plot them, we set  $q = 2$ ,  $r_0 = 1$  and  $\theta = \frac{\pi}{2}$ . Geodesics with  $b < b_c$ ,  $b = b_c$  and  $b > b_c$  are shown in red, blue, and green, respectively.

Universe 1, and the negative value to Universe 2. The impact parameter of the photon in circular orbit is

$$b_c = \varepsilon_0 \left. \frac{\sqrt{\Delta_r}}{f} \right|_{r=\pm qr_0} \quad (51)$$

for both universes.

In Figure 5, we show the graphs of  $V_{eff}$  for different values of the impact parameter  $b$ :  $b_c - 0.03 = 0.21424621627637944$ ,  $b_c = 0.24424621627637944$  and  $b_c + 0.03 = 0.27424621627637946$ . To plot them, we set  $q = 2$ ,  $r_0 = 1$  and  $\theta = \frac{\pi}{2}$ . Observe that the red curve does not cross the  $r$ -axis, while the blue curve takes the  $r$ -axis at  $r = 2$ . The green curve crosses the  $r$ -axis twice at  $r = 1.163715451958726$  and  $r = 3.493509720447682$ . However,  $r = 3.493509720447682$  is the minimum value that  $r$  can take. This means that geodesics with  $b > b_c$  do not reach the wormhole throat, as seen in Figure 6. Geodesics with  $b = b_c$  also do not reach the wormhole throat because they arrive at  $r = 2$  and are trapped in a circular orbit. Only geodesics with  $b < b_c$  cross the wormhole throat to the other universe.

Similarly, this occurs for other values of  $\theta$ , as can be seen in Figure 7. Observe that the red geodesic ( $b < b_c$ ) arrives at the wormhole throat, while the blue geodesic ( $b = b_c$ ) is trapped in a circular orbit, and the green geodesic ( $b > b_c$ ) moves away from the wormhole throat. To plot these geodesics, we set  $q = 2$ ,  $r_0 = 1$  and  $\theta = \frac{\pi}{2}$ .

## X. TIDAL FORCES

Employing the framework presented in [7] and using the vacuum condition  $R_{\mu\nu} = 0$ , we can conclude that the Riemann tensor coincides with the Weyl tensor, i.e.  $R_{\mu\nu\alpha\beta} = C_{\mu\nu\alpha\beta}$ .

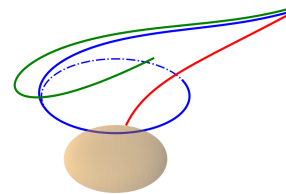


FIG. 7: Evolution of geodesics with distinct values of the impact parameter  $b$ . To plot them, we set  $q = 2$ ,  $r_0 = 1$  and  $\theta = \frac{\pi}{4}$ . Geodesics with  $b < b_c$ ,  $b = b_c$  and  $b > b_c$  are shown in red, blue, and green, respectively.

On the other hand, the geodesic deviation equation takes the form

$$\frac{D^2}{d\tau^2} \xi^\beta = R^\mu{}_{\alpha\beta\sigma} u^\alpha \xi^\beta u^\sigma,$$

where  $\tau$  denotes an affine parameter along the fiducial geodesic and  $D/d\tau = u^\mu \nabla_\mu$  represents the covariant derivative along that geodesic. This formulation guaran-

tees that the relative acceleration between neighboring freely falling particles is a tensorial quantity and, therefore, independent of the choice of observer. Therefore, we can consider the projections of  $R_{\mu\alpha\nu\beta}u^\alpha u^\beta = C_{\mu\alpha\nu\beta}u^\alpha u^\beta$  along the  $\{\text{preferred spatial or radial } s^\mu, \text{ axial } b^\mu, \text{ and polar directions } e^\mu\}$ :

$$\begin{aligned} u &= \left(1/\sqrt{f}, 0, 0, 0\right)^T, \\ s &= \left(0, \sqrt{f}/\Delta^{\ell/2}, 0, 0\right)^T, \\ e &= \left(0, 0, \sqrt{f/\Delta_r}/\Delta^{\ell/2}, 0\right)^T, \\ b &= \left(0, 0, 0, \sqrt{f/\Delta_r}/\sin\theta\right)^T. \end{aligned}$$

In this solution, the Newman–Penrose null tetrad obtained from a diagonal orthonormal frame coincides with the observer-adapted geometric NP tetrad constructed from  $(u^\mu, s^\mu, e^\mu, b^\mu)$ . This follows from the spacetime’s static nature and the fact that  $g_{tt}$  depends only on the radial coordinate. The unit four-velocity of static observers is  $u^\mu \propto \partial_t$ , and their proper acceleration  $a_\mu$  is purely radial. The remaining spatial vectors  $b^\mu$  and  $e^\mu$  are determined by axial symmetry and orthogonality, aligning with  $\partial_\phi$  and  $\partial_\theta$ , respectively. Thus the geometrically selected orthonormal frame  $(u, s, e, b)$  is parallel to the coordinate-adapted diagonal frame  $(\partial_t, \partial_r, \partial_\theta, \partial_\phi)$ , and the associated null vectors  $l^\mu = (u^\mu + s^\mu)/\sqrt{2}$  and  $n^\mu = (u^\mu - s^\mu)/\sqrt{2}$  coincide in both constructions, up to normalization.

And the projections  $E_{MN} = C_{\mu\alpha\nu\beta}M^\mu N^\nu u^\alpha u^\beta$  where  $M, N \in \{s, e, b\}$  are:

$$\begin{aligned} E_{ss} &= \frac{fqr_0}{8\Delta_\theta^{\frac{q^2}{4}+2}} \Delta_r^{\frac{q^2}{4}-1} \left( r_0^2 \cos^2(\theta) ((q^2 - 4)r + 4qr_0) \right. \\ &\quad \left. - r((q^2 + 4)r_0^2 - 4qr_0r + 8r^2) \right), \end{aligned} \quad (52a)$$

$$\begin{aligned} E_{ee} &= -\frac{fqr_0}{8\Delta_\theta^{\frac{q^2}{4}+2}} \Delta_r^{\frac{q^2}{4}-1} \left( qr_0^2 \cos^2(\theta)(qr + 2r_0) \right. \\ &\quad \left. - r((q^2 + 4)r_0^2 - 2qr_0r + 4r^2) \right), \end{aligned} \quad (52b)$$

$$E_{bb} = -\frac{fqr_0}{4\Delta_\theta^{\frac{q^2}{4}+1}} (qr_0 - 2r) \Delta_r^{\frac{q^2}{4}-1}, \quad (52c)$$

$$E_{se} = E_{es} = \frac{fq\Delta_r^{\frac{1}{4}(q^2-2)}}{8\Delta_\theta^{\frac{q^2}{4}+2}} (q^2 + 4) r_0^3 \sin\theta \cos\theta \quad (52d)$$

and the remaining ones disappear.

Let’s begin by remembering that

- $s$  is the **radial** unit direction,
- $e$  is the **polar** unit direction,
- $b$  is the **azimuthal**.

*a. Azimuthal and mixed polar-radial tidal forces.* By analysing (52), we observe that  $E_{bb} = 0 \iff r = r_G = \frac{qr_0}{2}$ , and that  $E_{se} \propto \sin\theta \cos\theta$ . Consequently,  $E_{se} = 0$  for  $\theta = 0, \frac{\pi}{2}, \pi$ . In other words, at the wormhole throat the azimuthal tidal force vanishes, and the mixed radial–polar tidal component is zero along both the polar axis and the equatorial plane. Since  $E_{bb} \propto (qr_0 - 2r)$ , the azimuthal tidal component flips sign as one crosses the throat: for  $r > r_G$  we have  $(qr_0 - 2r) < 0$ , which implies  $E_{bb} > 0$ , whereas for  $r < r_G$  we obtain  $(qr_0 - 2r) > 0$ , leading to  $E_{bb} < 0$ . Consequently, the behavior of a small separation in the  $\phi$ -direction switches from focusing/compression to stretching/defocusing, or vice versa, depending on the sign convention.

*b. Radial and polar tidal forces.* Because we have  $E_{bb}(r_G, \theta) = 0$  for every  $\theta$ , and the vacuum tidal tensor is traceless, satisfying  $E_{ss} + E_{ee} + E_{bb} = 0$ , it follows that

$$E_{ee}(r_G, \theta) = -E_{ss}(r_G, \theta) \quad (\forall \theta).$$

Thus, at the throat, any radial tidal effect is precisely balanced by an equal and opposite polar effect: radial stretching is accompanied by polar compression (and vice versa). On the other hand, we have  $E_{ss}(r_G, 0) = E_{ee}(r_G, 0) = 0$ , and analogously for  $\theta = \pi$ . In other words, the radial and polar tidal forces vanish at the throat exclusively along the polar axis. Consequently, this region constitute the most suitable axis for traversing the wormhole.

An illustration of the tidal forces is shown in Figure 8, where the case  $q = 2$  is considered, and the surface depicts the magnitude of each tidal force. The black curve corresponds to the tidal force at the wormhole throat, and we can clearly observe that the throat encompasses all the divergent anomalies of the surfaces. In other words, these anomalies lie inside the throat.

## XI. CONCLUSIONS

We used the flat subspaces method [33, 34] to obtain an exact solution  $\hat{g}$  to the EFE in vacuum, which depends on three constant parameters,  $r_0, q$  and  $s$ . Since  $\hat{g}$  is also valid for negative values of the radial coordinate  $r$ , we assumed  $r \in \mathbb{R}$ . In this way,  $\hat{g}$  describes a wormhole.

As mentioned earlier, the Komar mass is given by  $qr_0/2$ , so the parameter  $q$ , like  $r_0$ , is directly associated with the wormhole’s mass. In our construction, however,  $qr_0/2$  also coincides exactly with the throat radius, in other words, the geometric mass and the throat are identical. Moreover, an important point is that the parameter  $s$  is associated with the emergence of axial topological defects in our solution, although we have demonstrated that it does not lead to conical defects. Consequently, we set  $s = 0$  in our computations and have justified this choice, in particular, the metric  $\hat{g}$  is asymptotically flat only in the case  $s = 0$ . Similarly, this solution is static, with the NUT parameter and the Komar angular momentum both equal to zero.

In the case  $s = 0$ , it reduces to the ring wormhole. Furthermore, it has a singularity at  $(r, \theta) = (0, \frac{\pi}{2})$ , even if  $s \neq 0$ . This singularity can be geometrically interpreted as a ring of radius  $r_0$ .

We assumed that surfaces defined by constant  $t$  and  $r$  are surfaces of revolution. However, this occurs only for  $\frac{r}{r_0} \geq |\frac{q}{2}|$  or  $\frac{r}{r_0} \leq -|\frac{q}{2}|$ . Hence, we used the cut-paste method to construct wormholes. In Section VII, we determine the minimal surfaces. Only for  $\ell = 1$  and  $\ell = 2$  were we able to obtain a mathematical expression.

In Section VIII, we found that surfaces defined by constant  $t$  and  $\theta \in (0, \pi)$  are embedded in the Euclidean space  $\mathbb{R}^3$ . The profile curve (Figure 4a) is symmetric with respect to the  $\rho$ -axis, which implies that the surface (Figure 4b) is symmetric with respect to the plane  $z = 0$ .

The existence of solutions to the equations of motion is established in Section IX. We focused on solutions with constant  $\theta \in (0, \pi)$ , such solutions depends on the impact parameter  $b = \frac{J}{E}$ , where  $E$  is interpreted as the energy of the system and  $J$  as its angular momentum. The energy  $E$  is strictly positive, while  $J$  can take any real value. Only geodesics with an impact parameter  $b < b_c$  cross the wormhole throat to the other universe. Geodesics with  $b = b_c$  are trapped in a circular orbit, and geodesics with  $b > b_c$  move away from the wormhole throat.

Within the Newman–Penrose formalism, employing a Weyl-aligned null tetrad, and based on the asymptotic behavior, we discover that  $q$  is related to the mass. For  $q \neq 0$ , the corresponding spacetime is characterized by Petrov type I. In the asymptotic regime  $r \rightarrow \pm\infty$ , however, the algebraic structure of the Weyl tensor changes and the geometry tends to a Petrov type D spacetime.

In the same framework, we further show that the solution is static and does not support gravitational radiation. Due to its invariance under the reflection  $r \rightarrow -r$ , the geometry admits a consistent interpretation as a wormhole configuration. In the particular case  $q = 0$ , the metric becomes that of flat Minkowski spacetime, with both the mass and the throat (in the cut-and-paste construction) vanishing.

For this wormhole solution, the analysis of the tidal forces indicates that the safest region for traversability is located in the vicinity of the polar axis. This result is consistent with the findings reported in [4]. More importantly, we again conclude that this wormhole configuration satisfies the Wormhole Cosmic Censorship Conjecture (as discussed in [5]), since the throat effectively encloses all causal pathologies and trapped surfaces. Indeed, these pathologies and trapped regions are confined to  $r < qr_0/2$ , while the throat is precisely located at  $r_G = qr_0/2$ .

## ACKNOWLEDGEMENTS

This work was partially supported by CONAH-CyT México under grants A1-S-8742, 304001, 376127, 240512, FORDECYT-PRONACES grant No. 490769 and

I0101/131/07 C-234/07 of the Instituto Avanzado de Cosmología (IAC) collaboration (<http://www.iac.edu.mx/>).

# Appendices

## A. DIFFERENTIAL FORMS AND THE HODGE 2-FORM ON THE SURFACE $S_x$

Let the 2-surface:

$$S_x : \quad t = \text{const}, \quad r = \text{const}, \quad (\theta, \varphi) \in [0, \pi] \times [0, 2\pi]. \quad (53)$$

For sufficiently large values of  $|r|$ , this surface takes the form of a topological 2-sphere in the asymptotic region (for both the prolate and oblate coordinate systems). Hence, the limit  $r \rightarrow \infty$  (or  $r \rightarrow -\infty$  when a second asymptotic end exists) is equivalent to performing the integration over a large sphere at infinity. Consider now an antisymmetric 2-form  $H$ , whose covariant components satisfy  $H_{\mu\nu} = -H_{\nu\mu}$ . We employ the standard convention

$$(*H)_{\mu\nu} = \frac{1}{2}\sqrt{-g}\epsilon_{\mu\nu\alpha\beta}H^{\alpha\beta}, \quad H^{\alpha\beta} = g^{\alpha\gamma}g^{\beta\delta}H_{\gamma\delta}, \quad (54)$$

where

$$\sqrt{-g} = \frac{\Delta^\ell h \Delta_r \sin \theta}{f}.$$

Adopting the orientation convention  $\epsilon_{tr\theta\varphi} = +1$ , we can check (using antisymmetry and suitable index rearrangements) that  $\epsilon_{\theta\varphi tr} = +1$ . Consequently, from (54) it follows that  $(*H)_{\theta\varphi} = \sqrt{-g}H^{tr}$ . Noting that  $g^{rr} = \frac{f}{\Delta^\ell h}$  and  $g^{tt} = -1/f$ , we then obtain

$$(*H)_{\theta\varphi} = \sqrt{-g}g^{tt}g^{rr}H_{tr} = -\frac{\Delta_r \sin \theta}{f}H_{tr}. \quad (55)$$

Finally, if  $\Omega$  is a 2-form, then on  $S_x$  we have  $dt = dr = 0$ , and therefore

$$\int_{S_x} \Omega = \int_0^{2\pi} d\varphi \int_0^\pi d\theta (\Omega_{y\varphi}) \Big|_{t,r=\text{const}}. \quad (56)$$

Thus, to compute the integral of  $*H$  over  $S_x$ , it suffices to consider only the  $(*H)_{y\varphi}$  component.

## B. NEWMAN-PENROSE WEYL SCALARS

$$\Psi_4 = \Psi_0 = -\frac{fq(q^2+4)rr_0^3\sin^2(\theta)\Delta^{1-\frac{q^2}{4}}}{16\Delta_\theta^3}, \quad (57a)$$

$$\Psi_3 = -\Psi_1 = -\frac{fq(q^2+4)r_0^3\sin(2\theta)\Delta^{-\frac{q^2}{4}-\frac{1}{2}}}{32\Delta_\theta^{3/2}\Delta_r} \quad (57b)$$

$$\begin{aligned} \Psi_2 = & -\frac{fqr_0\Delta^{1-\frac{q^2}{4}}}{32\Delta_\theta^3} \left( r_0^2r((q^2-4)\cos(2\theta)-q^2-12) \right. \\ & \left. + 8qr_0r^2 + 8qr_0^3\cos^2(\theta) - 16r^3 \right). \quad (57c) \end{aligned}$$

$$\begin{aligned} \mathcal{I} = & \frac{q^2r_0^2\Delta_\theta^{-\frac{q^2}{2}-4}\Delta_r^{\frac{q^2}{2}-2}f^2}{1024} \left( 4(q^2+4)^2r^2r_0^4\sin^4(\theta) \right. \\ & + 3\left(r_0^2r((q^2-4)\cos(2\theta)-q^2-12) + 8qr_0r^2 \right. \\ & \left. \left. + 8qr_0^3\cos^2(\theta) - 16r^3\right)^2 + 4(q^2+4)^2r_0^4\sin^2(2\theta)\Delta_r \right), \quad (58a) \end{aligned}$$

$$\begin{aligned} \mathcal{J} = & -\frac{q^3r_0^3(qr_0-2r)\Delta_\theta^{-\frac{3q^2}{4}-4}\Delta_r^{\frac{3q^2}{4}-3}f^3}{1024} \dots \\ & \dots \left( 4r_0^2r^2((3q^2+4)\cos(2\theta)-7q^2-20) \right. \\ & - 2qr_0^3r((3q^2-4)\cos(2\theta)-3q^2-28) \\ & \left. + r_0^4((q^4+16)\cos(2\theta)-q^4-16q^2-16) \right) \quad (58b) \end{aligned}$$

$$+ 64qr_0r^3 - 64r^4). \quad (58c)$$

## A. Asymptotic behaviour

Within the Newman–Penrose framework, the leading asymptotic behavior of the Weyl scalars captures the dominant gravitational “Coulomb” contribution, any radiative terms, and higher multipole corrections. For our four-dimensional, vacuum, stationary spacetime, we consider the asymptotic limit as  $r \rightarrow \pm\infty$ , from which we obtain the approximations given in (59a).

$$\Delta_r \approx r^2, \quad \Delta_\theta \approx r^2, \quad \Delta \approx 1.$$

and

$$f_{\pm\infty} \approx e^{\pm q\pi/2}$$

therefore, (57a) takes the form:

$$\Psi_4 = \Psi_0 = \mp f_{\pm\infty} \frac{qlr_0^3\sin^2\theta}{4r^5}, \quad (59a)$$

$$\Psi_3 = -\Psi_1 = \mp f_{\pm\infty} \frac{qlr_0^3\sin 2\theta}{8r^5} \quad (59b)$$

$$\Psi_2 = \pm f_{\pm\infty} \frac{qr_0}{2r^3}. \quad (59c)$$

where  $\Xi_{\pm\infty} > 0$  denotes a dimensionless constant,  $q \in \mathbb{R}$  is a dimensionless parameter, and  $r_0$  is a constant. For the invariants denoted by  $\mathcal{I}$  and  $\mathcal{J}$ , we obtain the following result

$$\mathcal{I} \approx \frac{3(f_{\pm\infty})^2q^2r_0^2}{4r^6}, \quad (60a)$$

$$\mathcal{J} \approx \mp \frac{(f_{\pm\infty})^3q^3r_0^3}{8r^9}. \quad (60b)$$

It is straightforward to verify that, upon applying  $27\mathcal{J}^2$  and  $\mathcal{I}^3$ , we obtain the expression

$$\mathcal{I}^3 = 27\mathcal{J}^2 \approx \frac{27(f_{\pm\infty})^6q^6r_0^6}{64r^{18}}. \quad (61)$$

- 
- [1] Adamo, T.M., Kozameh, C.N., Newman, E.T., 2009. Null Geodesic Congruences, Asymptotically Flat Space-Times and Their Physical Interpretation. *Living Rev. Rel.* 12, 6. doi:doi:10.12942/lrr-2009-6, [arXiv:0906.2155](https://arxiv.org/abs/0906.2155).
- [2] Ashtekar, A., Krishnan, B., 2004. Isolated and dynamical horizons and their applications. *Living Rev. Rel.* 7, 10. doi:doi:10.12942/lrr-2004-10, [arXiv:gr-qc/0407042](https://arxiv.org/abs/gr-qc/0407042).
- [3] Bixano, L., Matos, T., 2025a. Einstein-Maxwell-dilaton wormholes that meet the energy conditions. *Phys. Rev. D* 111, 084056. doi:doi:10.1103/PhysRevD.111.084056, [arXiv:2502.07206](https://arxiv.org/abs/2502.07206).
- [4] Bixano, L., Matos, T., 2025b. On the Possibility of the Existence of Wormholes in Nature [arXiv:2505.20167](https://arxiv.org/abs/2505.20167).
- [5] Bixano, L., Sarmiento-Alvarado, I.A., Matos, T., 2025. A brief review of wormhole cosmic censorship. *Axioms* 14. URL: <https://www.mdpi.com/2075-1680/14/11/831>, doi:doi:10.3390/axioms14110831.
- [6] Bronnikov, K.A., 1973. Scalar-tensor theory and scalar charge. *Acta Phys. Polon. B* 4, 251–266.
- [7] Carroll, S.M., 2019. *Spacetime and Geometry*. Cambridge University Press. doi:doi:10.1017/9781108770385.
- [8] Clément, G., Gal'tsov, D., 2023. Rotating traversable wormholes in Einstein-Maxwell theory. *Phys. Lett. B* 838, 137677. doi:doi:10.1016/j.physletb.2023.137677, [arXiv:2210.08913](https://arxiv.org/abs/2210.08913).
- [9] De Falco, V., Battista, E., Capozziello, S., De Laurentis, M., 2021. Reconstructing wormhole solutions in curvature based Extended Theories of Gravity. *Eur. Phys. J. C* 81, 157. doi:doi:10.1140/epjc/s10052-021-08958-4, [arXiv:2102.01123](https://arxiv.org/abs/2102.01123).
- [10] Deshpande, R., Lunin, O., 2023. Charged wormholes in higher dimensions. *Nucl. Phys. B* 996, 116355. doi:doi:10.1016/j.nuclphysb.2023.116355, [arXiv:2212.11962](https://arxiv.org/abs/2212.11962).
- [11] Dzhunushaliev, V.D., 1998. Multidimensional geometrical model of the renormalized electrical charge with

- splitting off the extra coordinates. *Mod. Phys. Lett. A* 13, 2179–2186. doi:doi:10.1142/S021773239800231X, arXiv:gr-qc/9807080.
- [12] Einstein, A., Rosen, N., 1935. The particle problem in the general theory of relativity. *Phys. Rev.* 48, 73–77. URL: <https://link.aps.org/doi/10.1103/PhysRev.48.73>, doi:doi:10.1103/PhysRev.48.73.
- [13] Ellis, H.G., 1973. Ether flow through a drainhole: A particle model in general relativity. *Journal of Mathematical Physics* 14, 104–118. URL: <https://doi.org/10.1063/1.1666161>, doi:doi:10.1063/1.1666161.
- [14] Friedman, J.L., Schleich, K., Witt, D.M., 1993. Topological censorship. *Phys. Rev. Lett.* 71, 1486–1489. doi:doi:10.1103/PhysRevLett.71.1486, arXiv:gr-qc/9305017. [Erratum: *Phys.Rev.Lett.* 75, 1872 (1995)].
- [15] Gibbons, G.W., Volkov, M.S., 2016. Ring wormholes via duality rotations. *Phys. Lett. B* 760, 324–328. doi:doi:10.1016/j.physletb.2016.07.012, arXiv:1606.04879.
- [16] Gourgoulhon, E., Jaramillo, J.L., 2006. A 3+1 perspective on null hypersurfaces and isolated horizons. *Phys. Rept.* 423, 159–294. doi:doi:10.1016/j.physrep.2005.10.005, arXiv:gr-qc/0503113.
- [17] Hans, S., Dietrich, K., MacCallum, M., Hoenselaers, C., Herlt, E., 2009. *Exact Solutions of Einstein’s Field Equations*. 2nd edition ed., Cambridge University Press. doi:doi:https://doi.org/10.1017/CBO9780511535185.
- [18] Hayward, S.A., 1994. Spin coefficient form of the new laws of black hole dynamics. *Class. Quant. Grav.* 11, 3025–3036. doi:doi:10.1088/0264-9381/11/12/016, arXiv:gr-qc/9406033.
- [19] Hochberg, D., Visser, M., 1997. Geometric structure of the generic static traversable wormhole throat. *Phys. Rev. D* 56, 4745–4755. doi:doi:10.1103/PhysRevD.56.4745, arXiv:gr-qc/9704082.
- [20] Hochberg, D., Visser, M., 1998a. Dynamic wormholes, anti-trapped surfaces, and energy conditions. *Phys. Rev. D* 58, 044021. doi:doi:10.1103/PhysRevD.58.044021, arXiv:gr-qc/9802046.
- [21] Hochberg, D., Visser, M., 1998b. The Null energy condition in dynamic wormholes. *Phys. Rev. Lett.* 81, 746–749. doi:doi:10.1103/PhysRevLett.81.746, arXiv:gr-qc/9802048.
- [22] Israel, W., 1966. Singular hypersurfaces and thin shells in general relativity. *Nuovo Cim. B* 44S10, 1. doi:doi:10.1007/BF02710419. [Erratum: *Nuovo Cim.B* 48, 463 (1967)].
- [23] Komar, A., 1959. Covariant conservation laws in general relativity. *Phys. Rev.* 113, 934–936. doi:doi:10.1103/PhysRev.113.934.
- [24] Lobo, F.S.N., Oliveira, M.A., 2009. Wormhole geometries in  $f(R)$  modified theories of gravity. *Phys. Rev. D* 80, 104012. doi:doi:10.1103/PhysRevD.80.104012, arXiv:0909.5539.
- [25] Lü, H., Mei, J., 2008. Ricci-flat and charged wormholes in five dimensions. *Physics Letters B* 666, 511–516. doi:doi:10.1016/j.physletb.2008.07.100.
- [26] Maartens, R., Bassett, B.A., 1998. Gravitoelectromagnetism. *Class. Quant. Grav.* 15, 705. doi:doi:10.1088/0264-9381/15/3/018, arXiv:gr-qc/9704059.
- [27] van de Meent, M., 2013. Geometry of massless cosmic strings. *Phys. Rev. D* 87, 025020. doi:doi:10.1103/PhysRevD.87.025020, arXiv:1211.4365.
- [28] Morris, M.S., Thorne, K.S., 1988. Wormholes in space-time and their use for interstellar travel: A tool for teaching general relativity. *Am. J. Phys.* 56, 395–412. doi:doi:10.1119/1.15620.
- [29] Nedkova, P.G., Yazadjiev, S.S., 2011. On the Thermodynamics of 5D Black Holes on ALF Gravitational Instantons. *Phys. Rev. D* 84, 124040. doi:doi:10.1103/PhysRevD.84.124040, arXiv:1109.2838.
- [30] Newman, E., Penrose, R., 1962. An Approach to gravitational radiation by a method of spin coefficients. *J. Math. Phys.* 3, 566–578. doi:doi:10.1063/1.1724257.
- [31] Pirani, F.A.E., 1957. Invariant formulation of gravitational radiation theory. *Phys. Rev.* 105, 1089–1099. doi:doi:10.1103/PhysRev.105.1089.
- [32] Sarmiento-Alvarado, I.A., Bixano, L., Matos, T., 2025a. Wormholes exact solutions in high dimensions general relativity. URL: <https://arxiv.org/abs/2511.12392>, arXiv:2511.12392.
- [33] Sarmiento-Alvarado, I.A., Wiederhold, P., Matos, T., 2023. One-dimensional subspaces of the  $SL(n, \mathbb{R})$  chiral equations. *International Journal of Theoretical Physics* 62, 270. doi:doi:10.1007/s10773-023-05520-8.
- [34] Sarmiento-Alvarado, I.A., Wiederhold, P., Matos, T., 2025b. Flat subspaces of the  $SL(n, \mathbb{R})$  chiral equations. *General Relativity and Gravitation* 57, 132. doi:doi:10.1007/s10714-025-03467-1.
- [35] Vilenkin, A., 1985. Cosmic Strings and Domain Walls. *Phys. Rept.* 121, 263–315. doi:doi:10.1016/0370-1573(85)90033-X.
- [36] Visser, M., 1989. Traversable wormholes from surgically modified Schwarzschild space-times. *Nucl. Phys. B* 328, 203–212. doi:doi:10.1016/0550-3213(89)90100-4, arXiv:0809.0927.
- [37] Visser, M., 1996. *Lorentzian Wormholes: From Einstein to Hawking*. American Institute of Physics Melville, NY.
- [38] Zakhary, E., Mcintosh, C.B.G., 1997. A Complete Set of Riemann Invariants. *Gen. Rel. Grav.* 29, 539–581. doi:doi:10.1023/a:1018851201784.

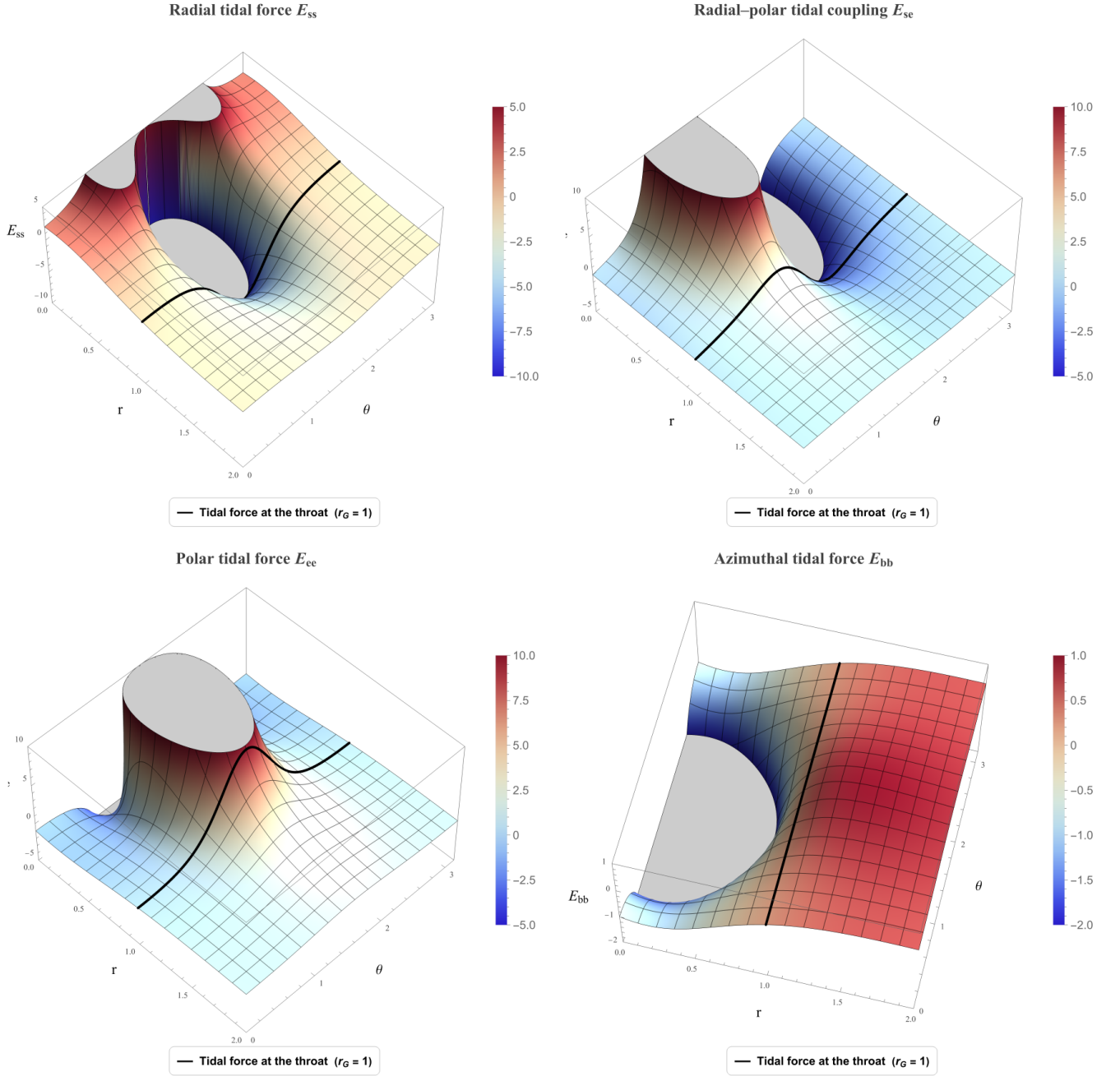


FIG. 8: Tidal forces are evaluated by fixing  $q = 2$  and  $r_0 = 1$  for all the cases of (52). The plotted surfaces represent the magnitude ( $z$ -Axis) of the wormhole, on each surface, a black curve is drawn indicating the tidal forces at the throat  $x_G = 1$  for any angle. It is evident that within the throat the magnitudes diverge, whereas outside the throat they remain finite and well-behaved.